

We are IntechOpen, the world's leading publisher of Open Access books Built by scientists, for scientists

6,900

Open access books available

186,000

International authors and editors

200M

Downloads

Our authors are among the

154

Countries delivered to

TOP 1%

most cited scientists

12.2%

Contributors from top 500 universities



WEB OF SCIENCE™

Selection of our books indexed in the Book Citation Index
in Web of Science™ Core Collection (BKCI)

Interested in publishing with us?
Contact book.department@intechopen.com

Numbers displayed above are based on latest data collected.
For more information visit www.intechopen.com



Long-Term Sea Level Variability in the Yellow Sea and East China Sea

Ying Xu, Mingsen Lin and Qunan Zheng

Additional information is available at the end of the chapter

<http://dx.doi.org/10.5772/intechopen.80735>

Abstract

Using the satellite altimeter maps of sea level anomaly (MSLA) and tidal gauge data, this chapter gives an investigation of the long-term sea level variability (SLV) and sea level rise (SLR) rate in the Yellow Sea (YS) and East China Sea (ECS). Correlation analysis shows that the satellite altimeter is effective and capable of revealing the coastal SLV. To investigate the regional correlation of SLV in the YS and ECS, tidal gauge station data are used as references. Based on the monthly maps of correlation coefficient (CC) of SLV at tidal stations with the gridded MSLA data, we find that the existence of Kuroshio decreases the correlation between the coastal and Pacific sea levels. The empirical mode decomposition (EMD) method is applied to derive the SLR trend on each MSLA grid point in the YS and ECS. According to the two-dimensional geographical distribution of the SLR rate, one can see that the sea level on the eastern side of the Kuroshio mainstream rises faster than that on the western side. Both the YS and ECS SLR rates averaged over 1993–2010 are slower than the globally averaged SLR rate. This implies that although the SLV in the two seas is affected by global climate change, it could be mostly influenced by local effects.

Keywords: East China Sea, Yellow Sea, sea level variability, empirical mode decomposition

1. Introduction

Long-term sea level variability (SLV) is critical for understanding global climate change. Meanwhile, accelerating sea level rise (SLR) in response to global warming has become a main issue that concerns the general public. Previous investigations have indicated that the SLR potentially affects human populations in coastal and island regions around the world and

changes natural environments like coastal and marine ecosystems [1–3]. As discussed in the fifth Intergovernmental Panel on Climate Change (IPCC) report, due to sea level rise projected throughout the twenty-first century and beyond, coastal systems and low-lying areas will increasingly experience adverse impacts such as submergence, coastal flooding and coastal erosion¹[4].

Global average sea levels rose 195 mm from 1870 to 2004 and showed an average annual rise of $1.44 \text{ mm}\cdot\text{a}^{-1}$ [5]. However, the recent SLR rate has reached about $3.00 \text{ mm}\cdot\text{a}^{-1}$ which is faster than previous estimation [6]. Researchers found that the distribution of SLV trend was not uniform around the world and the local characteristics of SLV trend were significant for prediction [7–8]. Eustatic changes, steric changes and geologic changes are the main influence factors of sea level variability [9]. To detect these changes as accurately as possible, researchers developed various methods. The analysis of tidal gauge data was the main approach for extracting sea level change signals before 1990s [10]. The combined analysis of satellite altimetry data and tidal gauge data has become an often-used tool for estimating global or regional SLV since 1990s [6, 11–14].

The applicability of satellite altimeter data in coastal sea areas has been validated by many works. Volkov et al. studied the performance of a corrected altimeter data over the north-west European shelf [15]. Their results demonstrated that although local tides effect should be further featured, the altimeter data can be effectively used in monitoring sea level variability over continental shelves. Cheng et al. jointly used satellite altimeter data and tide gauge data to predict the coastal sea level at the west and north coasts of the United Kingdom [16]. Their study showed tidal gauge data are consistent with satellite altimeter data for the annual change during 1993–2010. The annual amplitude correlation is 0.79 and the annual phase correlation is 0.80.

The coastal region off East China is vulnerable to SLR because of the geographical distribution of many low lands and river deltas. In addition, it is the most economically developed and densely populated region in China. Thus, the research on SLR and its impacts has been intensively investigated in China, particularly since 2000. From altimeter observations, Liu et al. calculated that the linear trend of SLR rate in the Yellow Sea (YS) was $5.05 \text{ mm}\cdot\text{a}^{-1}$ from 1992 to 2005 [17]. Zhan et al. used normal Morlet wavelet transform to investigate SLR trend in the China Seas and found that the SLR rate in the YS was $(4.01 \pm 0.49) \text{ mm}\cdot\text{a}^{-1}$ during 1992–2006 and the geographical distribution of the rate presented large differences [18]. Using 11 years altimeter data from 1992 to 2004, Qiao and Chen investigated the spatial-temporal SLV of the China Seas. Their results showed the major variation period was 1 year in the YS and East China Sea (ECS), with the SLR rate of the YS and ECS being 5.17 and $6.83 \text{ mm}\cdot\text{a}^{-1}$, respectively [19]. Liu et al. reported that the SLR rate reached $2.92 \text{ mm}\cdot\text{a}^{-1}$ in the southern part of the ECS (south of 30°N) [20]. The China Sea Level Bulletin 2010 indicates that the sea level in the Chinese Coastal Seas shows an overall fluctuating upward trend during the past 30 years, and that the SLR rate in both the YS and ECS was $2.8 \text{ mm}\cdot\text{a}^{-1}$ [21]. With wavelet transform method, Wang et al. studied the sea level change multi-scale cycle of the ECS. They found that the sea level in the ECS

¹**Foundation item:** The National Natural Science Foundation of China under contract No.41506207; the National Programme on Global Change and Air-Sea Interaction under contract No.GASI-02-SCS-YGST2-02.

showed upward trend and the SLR rate was up to $3.9 \text{ mm}\cdot\text{a}^{-1}$ between 1992 and 2009 [22]. Zuo et al. predicted the flooded area for the coastal regions of Shanghai City, Jiangsu Province and northern Zhejiang Province. Their results indicated that, on the condition of current SLR rate of $3.00 \text{ mm}\cdot\text{a}^{-1}$, the flooded area would be $64.1 \times 10^3 \text{ km}^2$ in 2050 and $67.8 \times 10^3 \text{ km}^2$ in 2080 [23]. Xu et al. studied the average SLR rate in the ECS between 1993 and 2010. The results showed the rising rate was $2.5 \text{ mm}\cdot\text{a}^{-1}$ and it was slower than global average [24].

In this chapter, we examine the SLV in the YS and ECS by using the combination of satellite altimeter data and tidal gauge data. Using the tidal gauge data as reference, the regional correlations of SLV in the YS and ECS are analyzed. Furthermore, long-term SLV trend and its two-dimensional distribution features in the entire YS and ECS are derived by using the empirical mode decomposition (EMD) method.

2. Data and method

2.1. Tidal gauge data

In-situ tidal gauge measures relative sea level variations with respect to a crustal reference point. It can provide a long and fine temporal resolution sea level record. However, there are two main problems when using tidal gauge data to investigate SLR. First, the crustal reference point itself may have vertical motions. Second, the limited spatial distribution of tidal stations has constrained the investigation of SLR, especially in the open seas.

In this chapter, we use the tidal gauge data from the University of Hawaii Sea Level Center (UHSLC), USA. It provides three kinds of sea level data including the research quality data, the fast delivery data (GLOSS/CLIVAR “fast delivery” data) and the SLP-Pac data (JCOMM Sea Level Program in the Pacific map data).

We select the daily research quality data, with six stations available near the coasts of the YS and ECS. Among all the data, only the time series with the same overlapping period as the satellite altimeter data are used. These daily data have been climatologically averaged to eliminate abnormal values. The locations and time spans of the six stations are listed in **Table 1**.

Station name	Latitude (N)	Longitude (E)	Time span	Station #
Laohutan	38°52′	121°41′	1993–1997	631
Shijiusuo	35°23′	119°33′	1993–1997	642
Lvsi	32°08′	121°37′	1993–1996	633
Kanmen	28°05′	121°17′	1993–1997	632
Xiamen	24°27′	118°04′	1993–1997	376
Shanwei	22°45′	115°21′	1993–1997	641

Table 1. Seven tidal stations in the Yellow Sea and East China Sea.

2.2. Satellite altimeter data

Being different from tidal gauge, satellite altimeter provides absolute measurements of sea level variations with respect to the Earth's center-of-mass. It gives independent measurements to investigate SLR with truly global coverage. The major disadvantage of satellite altimeter is its relatively shorter record duration compared to the tidal gauge data. Although the earlier altimeter data had some limitation due to orbit determination and measurement corrections, recent reprocessing of satellite data has shown great improvement and makes it possible to precisely measuring long-term SLVs.

The Archiving, Validation and Interpretation of Satellite Oceanographic data (AVISO) has distributed series of satellite altimetry products since 1992. Precise Orbit Ephemeris (POE) orbit and a centered computation time-window are applied to generate the delayed time (DT) products to achieve better accuracy. Therefore, the DT products are more suitable for sea level research.

In this chapter, we use daily global DT maps of sea level anomaly (MSLA) products as satellite altimeter data. The MSLA is a daily gridded data set which is provided on $(1/3)^\circ \times (1/3)^\circ$ Mercator grid for global coverage. With the daily resolution MSLA from October 14, 1992 to January 19, 2011, more data can be included in EMD trend extraction. And this helps us extract the trend more accurately.

2.3. Empirical mode decomposition

There are two kinds of models for investigation and prediction of SLR trend: numerical models based on physical processes and statistical models based on long-term observations [25]. As a physical approach, a hierarchy of numerical models have been used to estimate past changes and to project future changes in sea level for the IPCC. Meanwhile, a number of statistical approaches have been used to determine SLV, such as the empirical orthogonal function (EOF) analysis [6, 26], the regression method [14, 16], the semi-empirical method [27], spectral analysis [28] and the EMD analysis [29].

EMD introduced by Huang et al. [30] is used to extract sea level trend signals in this chapter. It is a powerful time series analysis tool, particularly for dealing with data from non-stationary and nonlinear processes. The EMD method, in contrast to almost all the other methods, is empirical, intuitive, direct and adaptive [31]. It is based on the assumption that time series data consist of different simple intrinsic modes of oscillations. Each of these linear or nonlinear modes is represented by an intrinsic mode function (IMF), which can have a variable amplitude and frequency as a function of time. Thus, EMD depends on the nature of the data sets. With the specific definition for the IMF and repeated siftings, one can decompose any function into IMFs, and the residue should be a trend.

In this chapter, the sea level data on each MSLA grid point can be describe as a time series function $x(t)$. The sifting process is shown in **Figure 1**.

During the first EMD sifting process, we identify all the local maxima and minima, and then use a cubic spline line to generate upper and lower envelopes. The mean of the upper and

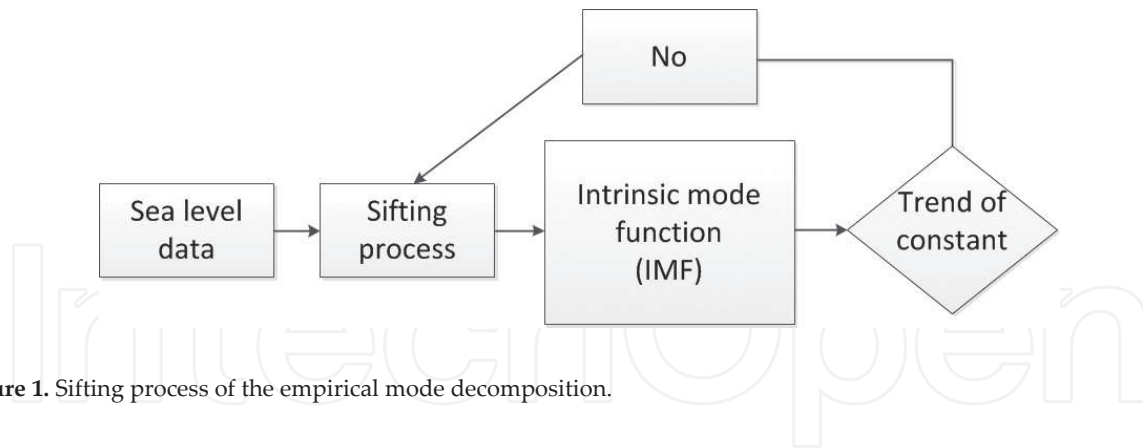


Figure 1. Sifting process of the empirical mode decomposition.

lower envelopes is designated as m_1 , and the difference between the data $x(t)$ and m_1 is the first component h_1 ,

$$h_1 = x(t) - m_1 \quad (1)$$

In the subsequent sifting processes, h_1 can be treated as the data, then

$$h_{11} = h_1 - m_{11} \quad (2)$$

After sifting process being repeated in this manner, when h_{1k} meets the specific definition of the IMF, h_{1k} becomes an IMF, that is,

$$h_{1k} = h_{1(k-1)} - m_{1k} \quad (3)$$

Then, the first IMF is designated as

$$c_1 = h_{1k} \quad (4)$$

Overall, c_1 should contain the finest scale of the shortest period component of the sea level signal. We empirically select n as the number of IMFs. Thus, the sifting process will stop when the number of IMFs is higher than n ,

$$n = \log_2(N) - 1 \quad (5)$$

where N is the number of sea level data. Thus, a decomposition of a MSLA grid-point data into n -empirical modes is achieved, and a residue r_n is obtained which can be the mean sea level trend. Finally, $x(t)$ is represented by

$$x(t) = \sum_{j=1}^n c_j + r_n \quad (6)$$

where IMF and trend are denoted as c_1, \dots, c_n and r_n , respectively. **Figure 2** shows the EMD analysis of the sea level on a MSLA grid point.

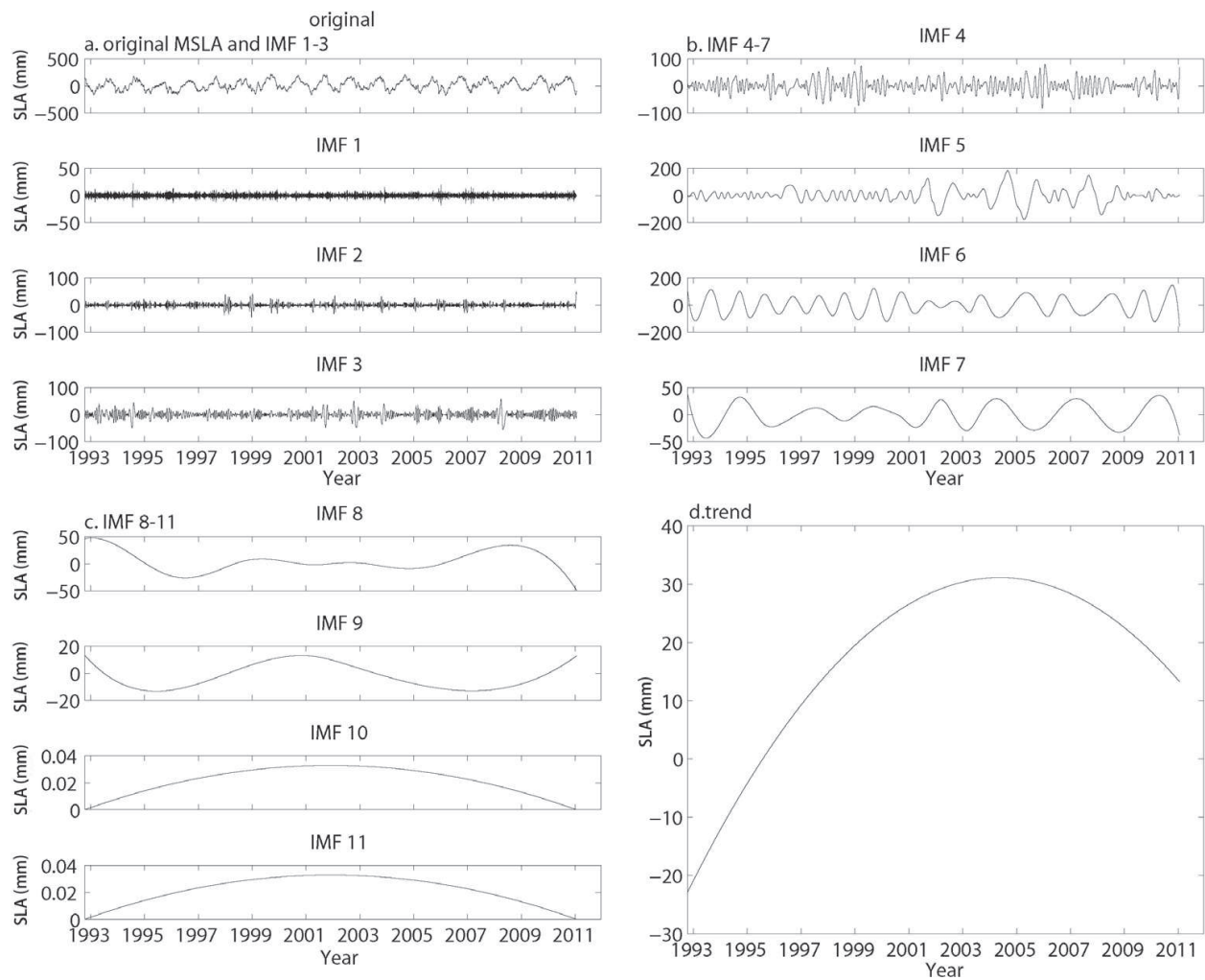


Figure 2. The EMD results at a MSLA grid point. The original is raw tidal gauge data, and IMFs 1–11 are the intrinsic oscillating modes. The trend is the SLR trend of a MSLA grid point from October 14, 1992 to January 19, 2011.

3. Regional correlation of sea level variability

3.1. Validation of maps of sea level anomaly

To accurately derive SLV and the trend, it is necessary to validate the applicability of MSLA in the YS and SCS. We calculate the correlation coefficient (CC) between tidal gauge data and the closest MSLA grid-point data. Both data sets are monthly-averaged to eliminate short-term fluctuations. With a maximum distance of 0.5' between the two types of data, the CCs at Laohutan, Shijiusuo, Lvsi, Kanmen, Xiamen and Shanwei stations are 0.89, 0.40, 0.65, 0.73, 0.79 and 0.81, respectively. The CC of Shijiusuo is relatively low but still in the moderate interval (0.30–0.50). The correlation suggests that satellite MSLA data are effective in sea level monitoring and research in the YS and ECS. **Figure 3** shows the CCs, the curves of the monthly-averaged sea level data and the closest MSLA grid-point data of the seven tidal stations.

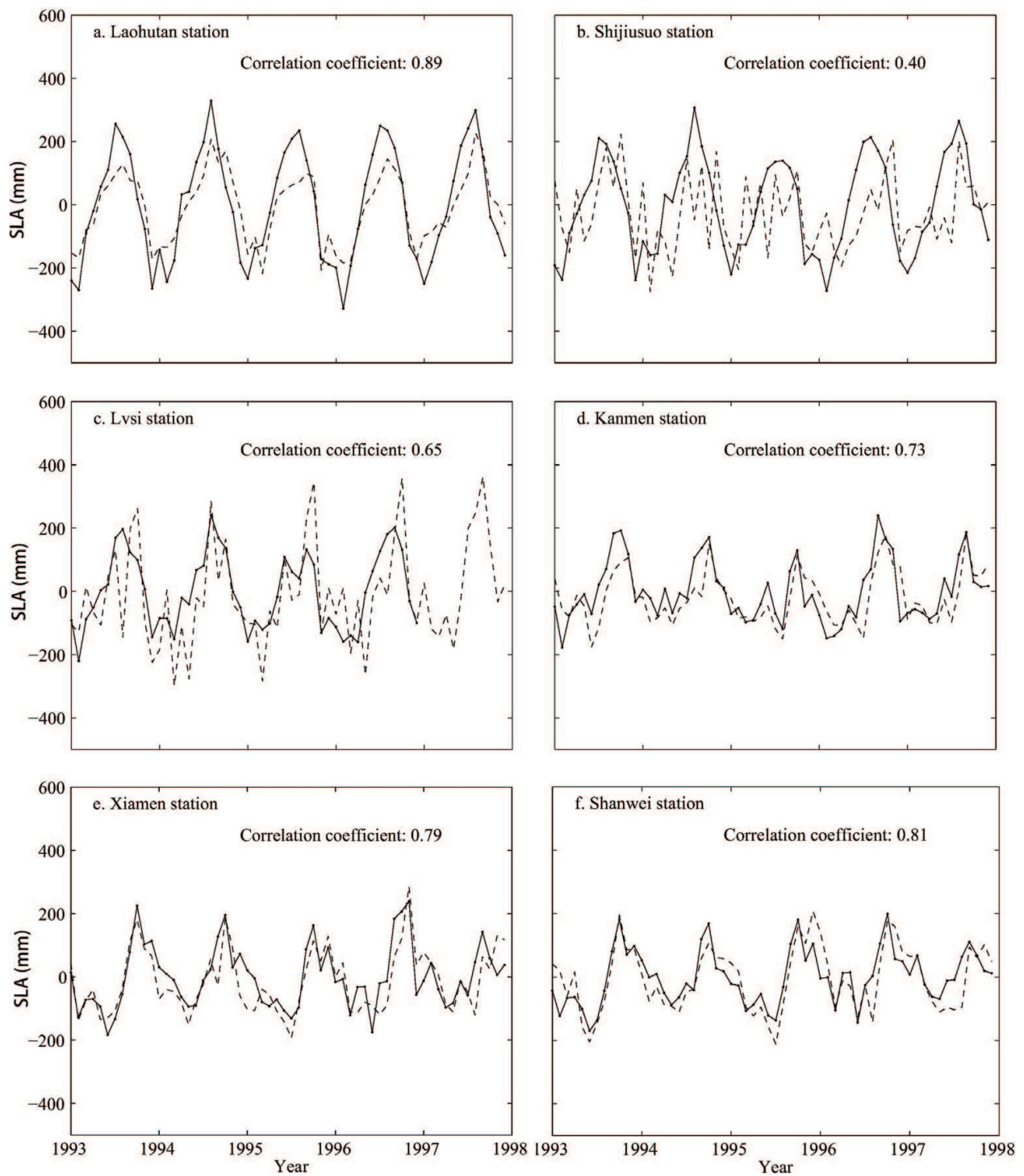


Figure 3. The correlation coefficient with gauge data at the most closest MSLA point of the Laohutan (a), Shijiusuo (b), Lvsi (c), Kanmen (d), Xiamen (e) and Shanwei (f) stations. Solid line is the monthly-averaged sea level data of a tidal station, and dashed line is the monthly-averaged data of the closest MSLA grid point to a selected station.

3.2. Regional correlation of sea level variability in the Yellow Sea

To study the geographical distribution features of the correlation of SLV between tidal gauge and MSLA points in the YS, we employ correlation analysis between the Laohutan, Shijiusuo

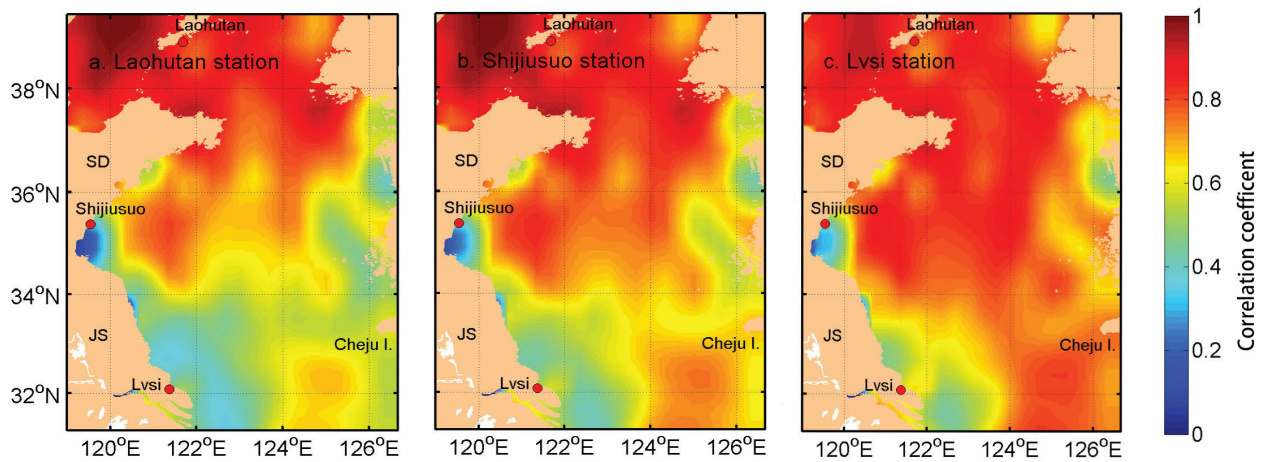


Figure 4. Monthly maps of correlation coefficient (CC) of SLV at Laohutan Station (a), Shijiusuo Station (b) and Lvsi Station (c) with that in the Yellow Sea. SD: Shandong Province; JS: Jiangsu Province.

and Lvsi stations and all the MSLA grid points in the entire YS. With this method, tidal gauge data are used as references to investigate the monthly regional correlation of SLV in the YS.

Figure 4 shows that the SLV at Laohutan station is highly correlated ($0.70 < CC < 0.80$) with that in its adjacent coastal region and the northern YS. The correlations of SLV at Shijiusuo and Lvsi stations with its adjacent coastal region is low ($0.20 < CC < 0.35$), but they are high ($0.7 < CC < 0.85$) with the northern, central and south-eastern regions of the YS. All three panels in **Figure 4** show that the SLV in northern, central and south-eastern regions of the YS (the open sea of the YS) is coherent. The SLV along the western coastal region of the YS also shows coherence between the two data sets.

The circulation in the YS is mainly composed of coastal ocean current system (west coastal current and east coastal current) and the open sea current system (Yellow Sea warm current) and Yellow Sea cold water mass circulation [32–33]. The distribution of CCs indicates on the monthly scale, the SLV in the YS is dominated by open sea and coastal ocean current systems of the YS, respectively.

3.3. Regional correlation of sea level variability in the East China Sea

Similarly, **Figure 5** is the monthly maps of the CC between the four tidal stations and the entire study area of the ECS. Using Lvsi station as reference, the result (**Figure 5a**) shows that the SLV in the northern and central regions of the ECS is highly correlated ($CC > 0.80$). While it is weakly correlated ($0.50 < CC < 0.70$) with the coastal ocean, and negatively correlated with the coastal seas of Fujian and Guangdong Province. At Kanmen Station (**Figure 5b**), we find a similar signature with Lvsi station. The highly correlated region ($CC > 0.80$) is mainly located in the northern and central regions of the ECS. However, the CCs in coastal regions of **Figure 5b** ($CC > 0.7$) are higher than **Figure 5a**. At Xiamen (**Figure 5c**) and Shanwei Station (**Figure 5d**), the highest correlation region ($CC > 0.80$) is located in the coastal seas of Zhejiang, Fujian and Guangdong province. And the CCs with the northern and central regions of the ECS are relatively weak. The Kuroshio can be clearly identified in all the panels of **Figure 5**. And the correlation show different characteristics on the left-hand side and the right-hand side of the Kuroshio core.

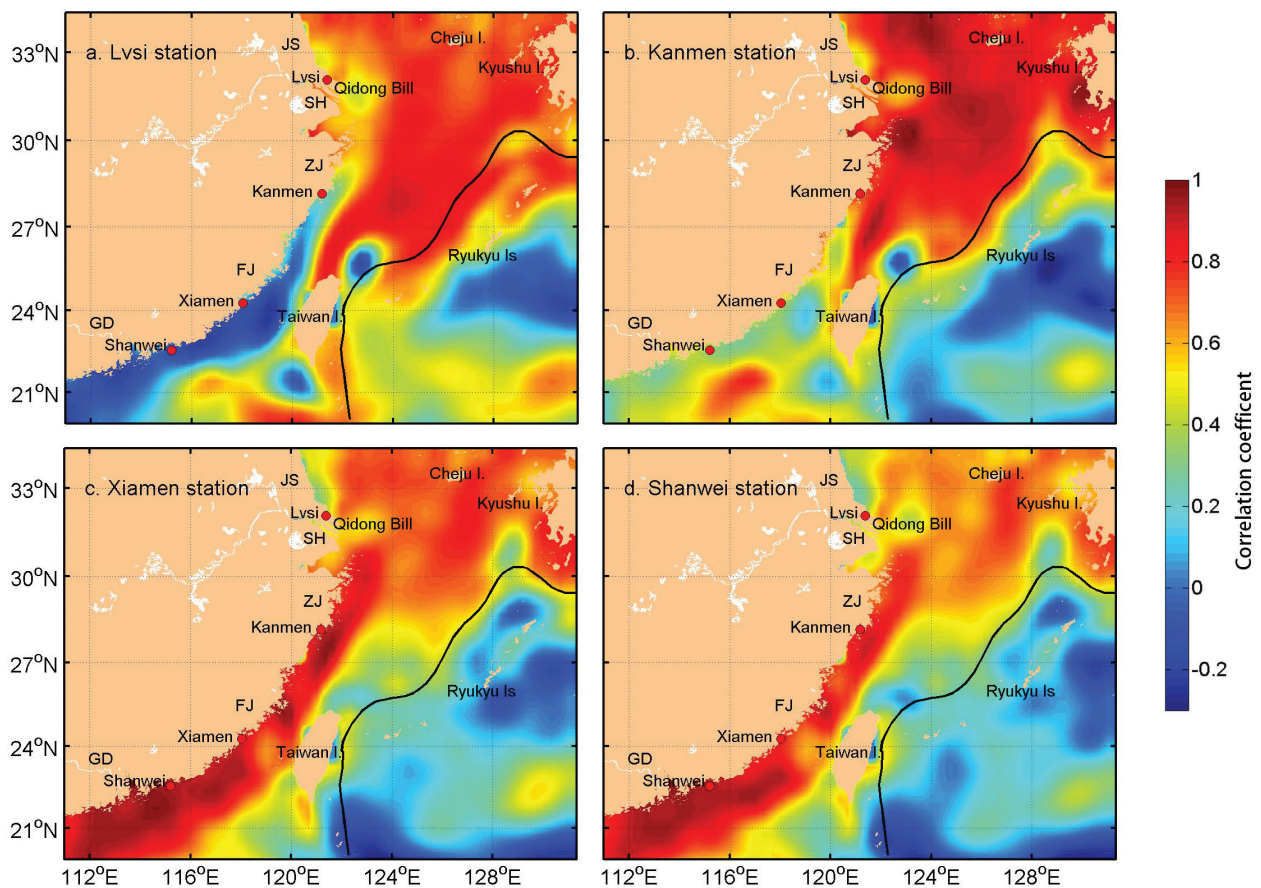


Figure 5. Monthly maps of correlation coefficient of SLV at Lvsu Station (a), Kanmen Station (b), Xiamen Station (c) and Shanwei Station (d) with the grid-point data in the East China Sea. JS: Jiangsu Province; ZJ: Zhejiang Province; FJ: Fujian Province and GD: Guangdong Province.

The circulation in the ECS is mainly composed of warm current (the Kuroshio) and coastal ocean current system (coastal current of Zhejiang and Fujian) [32–33]. The distribution of CCs indicates that the major water mass and the coastal regions in the ECS are dominated by different mechanism on the monthly scale. The Kuroshio blocks the link of SLV between the left-hand and right-hand of its flow core.

4. Long-term sea level variability trend

4.1. Two-dimensional distribution features of trend in the Yellow Sea

Sea level trend at a few MSLA grid points cannot give the detailed pattern in the YS. To better understand the geographical distribution of SLR trend, we calculate the annual-average SLR rate and generate the maps of the rate in the YS from 1993 to 2010, from 1993 to 1998 and from 1999 to 2010, respectively. **Figure 6** shows the distributions in the three phases.

Overall, the annual-average SLR rate in the YS between 1993 and 2010 was (1.03 ± 3.16) $\text{mm}\cdot\text{a}^{-1}$. The fastest SLR regions were located along the west coast and in the southern part of

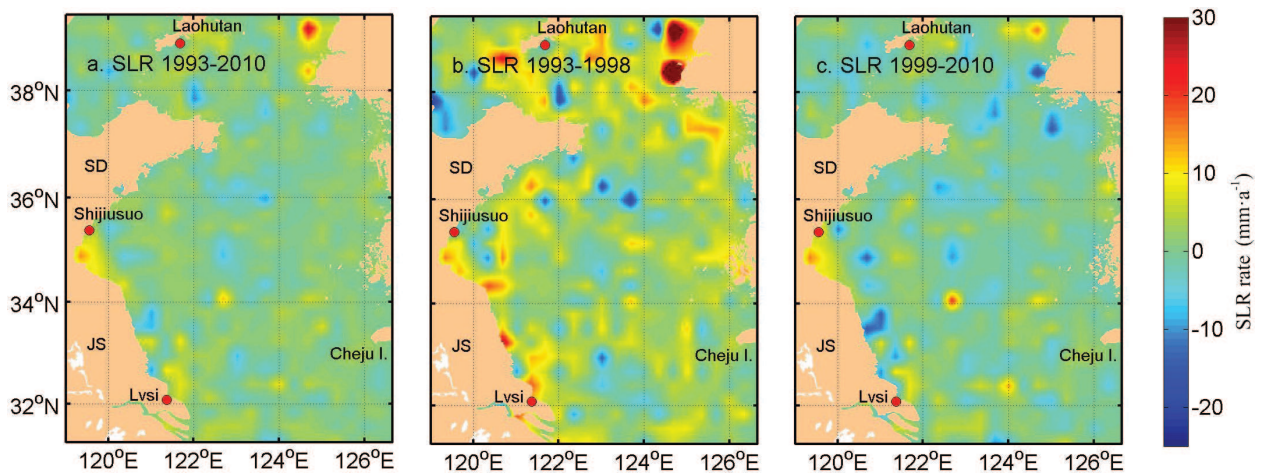


Figure 6. Distributions of SLR rates in the Yellow Sea obtained using the EMD: (a) 1993–2010, (b) 1993–1999 and (c) 1999–2010.

the YS. In the central part of the YS, the SLR rates were negative. The SLR rates from 1993 to 1998 and from 1999 to 2010 were $3.54 \pm 7.08 \text{ mm}\cdot\text{a}^{-1}$ and $-0.01 \pm 4.04 \text{ mm}\cdot\text{a}^{-1}$, respectively. The geographical distributions of the fastest SLR rates in the periods of 1993–1998 and 1999–2010 show similar characteristics to the period of 1993–2010. It is worth noting that the rate of SLR turned from positive to negative value since 1999.

4.2. Two-dimensional distribution features of the trend in the East China Sea

Figure 7 shows the geographical distribution of SLR rate in the ECS. Between 1993 and 2010, the annual-average SLR rate in the ECS was $2.50 \pm 3.64 \text{ mm}\cdot\text{a}^{-1}$. The SLR rates from 1993 to 1998 and from 1999 to 2010 were $4.08 \pm 6.95 \text{ mm}\cdot\text{a}^{-1}$ and $1.88 \pm 4.80 \text{ mm}\cdot\text{a}^{-1}$, respectively. However, the rate was neither uniformly nor simultaneously distributed in the ECS. We can see the rate on the right-hand side of the Kuroshio core was faster than on the left-hand side in all the panels of **Figure 7**. That may indicate the role of warm water transportation of the Kuroshio in SLR is not more important than the local processes in the ECS.

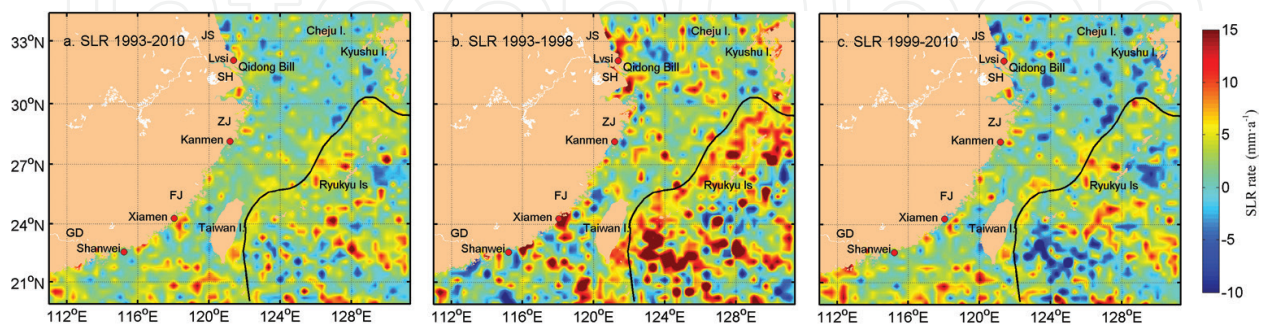


Figure 7. Distributions of SLR rates in the East China Sea obtained using from the EMD: (a) 1993–2010, (b) 1993–1999 and (c) 1999–2010.

5. Summary

In this chapter, we deal with long-term SLV in the YS and ECS using satellite altimeter MSLA data from 1992 to 2011, as well as data from six tidal gauges from 1996 to 1999. Major findings are summarized as follows.

(1) Using correlation analysis method, we first calculate the monthly-averaged correlation coefficients between the tidal gauge data and the closest MSLA grid-point data to validate the applicability of MSLA in the YS and ECS.

The results indicate that, in addition to Shijiusuo station where the CC is 0.40 (in the moderate interval), the CCs at the other five tidal station show high correlations. The maximum value of the correlation coefficients is 0.89 at Laohutan Station. These results confirm that using satellites to observe coastal SLV is effective and feasible when MSLA data is monthly-averaged.

(2) Furthermore, we apply the correlation analysis between MSLA and tidal gauge data in the YS and ECS. The regional correlation of SLV in the YS and ECS between the two data sets is investigated using the tidal station data as the reference.

For the YS, according to the correlation coefficient map, the monthly SLV in the northern, central and south-eastern regions of the YS (the open sea of the YS) and that along the western coastal region of the YS show coherence, respectively.

For the ECS, the monthly SLV in the northern and central regions of the ECS and that along the coastal regions of Zhejiang, Fujian and Guangdong province show coherence, respectively. The existence of the Kuroshio decreases the correlation or generates negative correlation between coastal sea level and Pacific sea level.

The geographical distributions of CCs show that the SLV in the YS and ECS are affected by the circulation systems on monthly scale. The Kuroshio acts like a barrier, which blocks the effect of the Pacific and global change.

(3) The EMD method is used to derive sea level trend in the YS and ECS. Then the SLR rate is calculated based on the trend, and its two-dimensional geographical distribution is investigated. The important findings are given below.

In the YS, the SLR rate turned from positive to negative value in 1999–2010, and the fastest SLR regions were located along the west coast and in the southern region of the YS. In the ECS, the SLR rate significantly slowed down in 1999–2010, and the sea level on the right-hand side of the Kuroshio core rose distinctly faster than on the left-hand side of the Kuroshio. This further supports the barrier effect of the Kuroshio in the ECS.

A recent study shows that the global warming has paused while the deep ocean takes the heat instead [34]. In this study, we found the SLR rate after 1999 also slowed down significantly in the YS and ECS. This kind of change shows that SLR in YS and ECS is affected by global climate change. Moreover, the SLR rates in the YS ($1.03 \pm 3.16 \text{ mm}\cdot\text{a}^{-1}$) and in the ECS ($2.50 \pm 3.64 \text{ mm}\cdot\text{a}^{-1}$)

during 1993–2010 are lower than the global average ($3.00 \text{ mm}\cdot\text{a}^{-1}$). The lower rate than the global average indicates that local system effects play important roles in the SLR in the YS and ECS.

Both SLR and circulation system in the YS and ECS are complicated. There still are no answers to many critical questions about the ocean dynamics in the YS and ECS. The subject on the SLR in the YS and ECS remains a research focus under debate. We hope that this study will bring some useful information to this debate.

Acknowledgements

We thank to the dedications of MSLA data from AVISO/CNES (<http://www.aviso.altimetry.fr/en/data.html>) and tidal gauge sea level data from UHSLC (University of Hawaii Sea Level Center). We also wish to thank the Department of Atmospheric and Oceanic Science, University of Maryland for resources while the lead author was a visiting scholar there.

Author details

Ying Xu^{1*}, Mingsen Lin¹ and Quanan Zheng²

*Address all correspondence to: xuying@mail.nsoas.org.cn

1 National Satellite Ocean Application Service, Key Laboratory of Space Ocean Remote Sensing and Application, State Oceanic Administration, Beijing, China

2 Department of Atmospheric and Oceanic Science, University of Maryland, MD, USA

References

- [1] Bindoff NL, Willebrand J, Artale V, Cazenave A, Gregory J, Gulev S, et al. Observations: oceanic climate change and sea level. In: Labeyrie L, Wratt D, editors. *Climate Change 2007: The Physical Science Basis. Contribution of Working Group I to the Fourth Assessment Report of the Intergovernmental Panel on Climate Change*. Cambridge, United Kingdom and New York, NY, USA: Cambridge University Press; 2007. pp. 385-432
- [2] Fischlin A, Midgley GF, Price JT, Leemans R, Gopal B, Turley C, et al. Ecosystems, their properties, goods and services. In: Cramer W, Diaz SM, editors. *Climate Change 2007: Impacts, Adaptation and Vulnerability. Contribution of Working Group II to the Fourth Assessment Report of the Intergovernmental Panel on Climate Change*. Cambridge: Cambridge University Press; 2007. pp. 211-272
- [3] Nicholls RJ, Cazenave A. Sea-level rise and its impact on coastal zones. *Science*. 2010; **328**(5985):1527-1520. DOI: 10.1126/science.1185782

- [4] Wong PP, Losada IJ, Gattuso J-P, Hinkel J, Khattabi A, McInnes KL, et al. Coastal systems and low-lying areas. In: Nicholls RJ, Santos F, editors. *Climate Change 2014: Impacts, Adaptation, and Vulnerability. Part A: Global and Sectoral Aspects. Contribution of Working Group II to the Fifth Assessment Report of the Intergovernmental Panel on Climate Change*. Cambridge, United Kingdom and New York, NY, USA: Cambridge University Press; 2014. pp. 361-409
- [5] Church JA, White NJ. A 20th century acceleration in global sea-level rise. *Geophysical Research Letters*. 2006;**33**(1):L01602. DOI: 10.1029/2005GL024826
- [6] Church JA, White NJ. Sea-level rise from the late 19th to the early 21st century. *Surveys in Geophysics*. 2011;**32**(4-5):585-602. DOI: 10.1007/s10712-011-9119-1
- [7] Cazenave A, Nerem RS. Present-day sea-level change observations and causes. *Reviews of Geophysics*. 2004;**42**(3):131-144. DOI: 10.1029/2003RG000139
- [8] Church JA, Gregory JM, Huybrechts P, Kuhn M, Lambeck K, Nhuan MT, et al. Changes in sea level. In: Douglas BC, Ramirez A, editors. *Climate Change 2001: The Scientific Basis, Contribution of Working Group I to the Third Assessment Report of the Intergovernmental Panel on Climate Change*. New York, NY, USA: Cambridge University Press; 2001. pp. 639-693
- [9] Carton JA, Giese BS, Grodsky SA. Sea level rise and the warming of the oceans in the simple ocean data assimilation (SODA) ocean reanalysis. *Journal of Geophysical Research*. 2005;**110**(C9):C09006. DOI: 10.1029/2004JC002817
- [10] Douglas BC. Global sea level acceleration. *Journal of Geophysical Research*. 1992;**97**(C8): 12699-12706. DOI: 10.1029/92JC01133
- [11] Cabanes C, Cazenave A, Le Provost C. Sea level rise during past 40 years determined from satellite and in situ observations. *Science*. 2001;**294**(5543):840-842. DOI: 10.1126/science.1063556
- [12] Mangiarotti S. Coastal sea level trends from TOPEX-poseidon satellite altimetry and tide gauge data in the mediterranean sea during the 1990s. *Geophysical Journal International*. 2007;**170**(1):132-144. DOI: 10.1111/j.1365-246X.2007.03424.x
- [13] Trisirisatayawong I, Naejie M, Simons W, Fenoglio-Marc L. Sea level change in the Gulf of Thailand from GPS-corrected tide gauge data and multi-satellite. *Global and Planetary Change*. 2011;**76**(3-4):137-151. DOI: 10.1016/j.gloplacha.2010.12.010
- [14] Dean RG, Houston JR. Recent sea level trends and accelerations: comparison of tide gauge and satellite results. *Coastal Engineering*. 2013;**75**(5):4-9. DOI: 10.1016/j.coastaleng.2013.01.001
- [15] Volkov DL, Larnicol G, Dorandeu J. Improving the quality of satellite altimetry data over continental shelves. *Journal of Geophysical Research*. 2007;**112**(C6):C06020. DOI: 10.1029/2006JC003765

- [16] Cheng YC, Andersen OB, Knudsen P. Integrating non-tidal sea level data from altimetry and tide gauges for coastal sea level prediction. *Advances in Space Research*. 2012;**50**(8):1099-1106. DOI: 10.1016/j.asr.2011.11.016
- [17] Liu GF, Ma HQ, Zhang GY. Trends and wavelet correlation analysis of sea level changes in the China Seas and the global area from satellite altimetry (In Chinese). *Science of Surveying and Mapping*. 2007;**32**(6):56-58. DOI: 10.3771/j.issn.1009-2307.2007.06.018
- [18] Zhan JG, Wang Y, Xu HZ, Hao XG, Liu LT. The wavelet analysis of sea level change in China Sea during 1992-2006 (In Chinese). *Acta Geodaetica et Cartographica Sinica*. 2008;**37**(4):438-443. DOI: 10.3321/j.issn:1001-1595.2008.04.007
- [19] Qiao X, Chen G. A preliminary analysis on the China Sea level using 11 years' TOPEX/Poseidon altimeter data (In Chinese). *Marine Sciences*. 2008;**32**(1):60-64. DOI: 1000-3096(2008)01-0060-05
- [20] Liu XY, Liu YG, Guo L, Gu YZ. Change of mean sea level of low-frequency on East China Sea and its relation with ENSO (In Chinese). *Journal of Geodesy and Geodynamics*. 2009;**29**(4):55-63. DOI: 1671-5942(2009)04-0055-09
- [21] State Oceanic Administration, People's Republic of China. China Sea Level Bulletin 2010 (In Chinese) [Internet]. 2011;**4**:22. Available from: http://www.soa.gov.cn/zwgk/hygb/zghpmb/201211/t20121105_5567.html
- [22] Wang GD, Kang JC, Han GQ, Liu C. Analysis and prediction of sea-level-change multi-scale cycle for East China Sea (In Chinese). *Advances in Earth Science*. 2011;**26**(6):678-684. DOI: 1001-8166(2011)06-0678-07
- [23] Zuo JC, Yang YQ, Zhang JL, Chen MX, Xu Q. Prediction of China's submerged coastal areas by sea level rise due to climate change. *Journal of Ocean University of China*. 2013;**12**(3):327-334. DOI: 10.1007/s11802-013-1908-3
- [24] Xu Y, Lin MS, Zheng QA, Ye XM, Li JY, Zhu BL. A study of long-term sea level variability in the East China Sea. *Acta Oceanologica Sinica*. 2015;**34**(11):109-117. DOI: 10.1007/s13131-015-0754-0
- [25] Baart F, Koningsveld MV, Stive MJF. Trends in sea-level trend analysis. *Journal of Coastal Research*. 2012;**28**(2):311-315. DOI: 10.2112/JCOASTRES-11A-00024.1
- [26] Church JA, White NJ, Coleman R, Lambeck K, Mitrovica JX. Estimates of the regional distribution of sea level rise over the 1950-2000 period. *Journal of Climate*. 2004;**17**(13):2609-2625. DOI: 10.1175/1520-0442(2004)017%3C2609:EOTRDO%3E2.0.CO;2
- [27] Rahmstorf S. A Semi-empirical approach to projecting future sea-level rise. *Science*. 2007;**315**(5810):368-370. DOI: 10.1126/science.1135456
- [28] Fenoglio-Marc L. Long-term sea level change in the mediterranean sea from multi-satellite altimetry and tide gauges. *Physics and Chemistry of the Earth, Parts A/B/C*. 2002;**27**(32-34):1419-1431. DOI: 10.1016/S1474-7065(02)00084-0

- [29] Ezer T. Sea level rise, spatially uneven and temporally unsteady: why the U. S. East Coast, the global tide gauge record, and the global altimeter data show different trends. *Geophysical Research Letters*. 2013;**40**(20):5439-5444. DOI: 10.1002/2013GL057952
- [30] Huang NE, Shen Z, Long SR, Wu MC, Shin HH, Zheng QA, et al. The empirical mode decomposition and the Hilbert spectrum for nonlinear and non-stationary time series analysis. *Proceedings of the Royal Society A: Mathematical, Physical and Engineering Sciences*. 1998;**454**(1971):903-995. DOI: 10.1098/rspa.1998.0193
- [31] Huang NE, Shen SSP, editors. *Hilbert-Huang Transform and Its Applications*. 1st ed. Tuck Link, Singapore: World Scientific Publishing Company; 2005. 324 p. DOI: 10.1142/5862
- [32] Guan BX. Patterns and structures of the currents in Bohai, Huanghai and East China Seas. *Oceanology of China seas*. 1994;**1**:17-26
- [33] Qiao FL, editor. *Regional Oceanography of China Seas-Physical Oceanography (In Chinese)*. Beijing, China: China Ocean Press; 2012. 481 p
- [34] Chen XY, Tung KK. Varying planetary heat sink led to global-warming slowdown and acceleration. *Science*. 2014;**345**(6199):897-903. DOI: 10.1126/science.1254937

